BEST AVAILABLE IMAGES

Defective images within this document are accurate representations of the original documents submitted by the applicant.

Defects in the images may include (but are not limited to):

- BLACK BORDERS
- TEXT CUT OFF AT TOP, BOTTOM OR SIDES
- FADED TEXT
- ILLEGIBLE TEXT
- SKEWED/SLANTED IMAGES
- COLORED PHOTOS
- BLACK OR VERY BLACK AND WHITE DARK PHOTOS
- GRAY SCALE DOCUMENTS

IMAGES ARE BEST AVAILABLE COPY.

As rescanning documents *will not* correct images, please do not report the images to the Image Problem Mailbox.

Transduction of murine cerebellar neurons with recombinant FIV and AAV5 vectors

Joseph M. Alisky,[1] Stephanie M. Hughes,[1] Sybille L. Sauter,[3] Douglas Jolly,[3] Thomas W. Dubensky Jr,[3] Patrick D. Staber,[1] John A. Chiorini[4] and Beverly L. Davidson,[1,2,CA]

Program in Gene Therapy, Departments of [1]Internal Medicine and [2]Neurology, University of Iowa College of Medicine, Iowa City, IA 52242; [3]Chiron Corporation, Center for Gene Therapy, San Diego, CA 92121-1204; [4]Gene Therapy and Therapeutics Branch, NIDCR, Bethesda, MD 20892, USA

[CA,1]Corresponding Author and Address

Received 23 May 2000; accepted 7 June 2000

Our data demonstrate that vectors derived from recombinant feline immunodeficiency virus (rFIV) and adeno-associated virus type 5 (rAAV5) transduce cerebellar cells following direct injection into the cerebellar lobules of mice. Both recombinant viruses mediated gene transfer predominantly to neurons, with up to 2500 and 1500 Purkinje cells transduced for rAAV5 or rFIV-based vectors, respectively. The vectors also transduced stellate, basket and Golgi neurons, with occasional transduction of granule cells and deep cerebellar nuclei. rAAV5 also spread outside the cerebellum to the inferior colliculus and ventricular epithelium, while rFIV demonstrated the ability to undergo retrograde transport to the physically close lateral vestibular nuclei. Thus, AAV5 and FIV-based vectors show promise for targeting neurons affected in the hereditary spinocerebellar ataxias. These vectors could be important tools for unraveling the pathophysiology of these disorders, or in testing factors which may promote neuronal survival. *NeuroReport* 11:2669–2673 © 2000 Lippincott Williams & Wilkins.

Key words: Axonal transport; Gene therapy; Purkinje cells

INTRODUCTION

Degenerative diseases of the cerebellum, such as the autosomal dominant spinocerebellar ataxias (SCA), are potentially amenable to gene therapy if sufficient numbers of the appropriate neuronal populations could be transduced. The SCAs can result from loss of Purkinje cells, inferior olivary and pontine neurons and, to a lesser extent, granule cells [1,2]. Onset is typically from the fifth to seventh decade of life, with degeneration occurring over a decade. The underlying genetic defect in several types of the SCA (SCA-1, SCA-2, SCA-3, and SCA-7) causes polyglutamine tract expansion and a toxic gain of function in the encoded protein [3,4]. Genes encoding neuroprotective sequences could in theory prevent or slow the degenerative process in these disorders.

Previous investigations of gene transfer in the cerebellum have been limited to replication-deficient adenovirus vectors (rAd). rAd expressing β-galactosidase injected into the cerebellar cortex of mice transduced precerebellar neurons in the brain stem [5,6]. This occurred via retrograde axonal transport of virons from mossy fiber terminals in the cortex back to neuronal soma. However, within the cortex itself mainly glia were transduced, with minimal transduction of Purkinje cells or other classes of neurons. Viral vectors that transduce cerebellar neurons directly would be preferable for use in the study of the spinal cerebellar ataxias, and for testing therapies in representative animal models [7,8].

Replication incompetent recombinant lentiviral vectors derived from human immunodeficiency virus (rHIV) or feline immunodeficiency virus (rFIV) show tropism for neurons *in vitro* [9] and *in vivo* when injected into the cerebrum [10]. The recombinant lentivirus vectors remain capable of infecting non-dividing cells when deleted of accessory proteins [11,12]. In recent studies, rHIV vectors pseudotyped with the vesicular stomatitis glycoprotein G (VSV-g) envelope protein mediated gene transfer to a large number of striatal neurons when injected into non-human primate brain, with no apparent decline in transgene expression throughout the three month study [13]. Similar results have been found with FIV-based lentivirus vectors [14].

Recombinant adeno-associated viruses (rAAV) have also been shown to mediate gene transfer to neurons when injected into the rodent cerebrum [15–19]. AAVs are DNA dependoviruses, requiring helper viruses for productive infections [20]. Six different AAV serotypes have been isolated (AAV1–AAV6), but only three have been tested for their transduction properties in mammalian brain: rAAV2, rAAV4, and rAAV5.

Earlier studies showed that vectors derived from AAV2 efficiently transduce neurons immediate to the site of administration [16,19]. More recently, we demonstrated that rAAV5-based vectors are capable of diffusion within the mouse striatum well beyond the injection site [19]. Similar to rAAV2 vectors, rAAV5 predominantly trans-

duced neurons in the hippocampus, cortex, striatum and medial septum. In this study we asked whether rAAV5 and rFIV could similarly transduce neurons in the cerebellum.

MATERIALS AND METHODS

Preparation of viral vectors: Both the rFIV and rAAV5 vectors have been described previously [11,19]. Briefly, the rFIV contained mutant vif and orf2 sequences inhibiting their expression, and expressed *Escherichia coli* β-galactosidase (cytoplasmic expression) driven off a cytomegalovirus promoter (rFIVβgal). The rAAV5 contained native AAV5 ITRs and was packaged using a three-plasmid transfection system, including one encoding AAV5 rep and cap [19,21]. The rAAV5 expresses nuclear targeted *E. coli* β-galactosidase from a Rous sarcoma virus promoter (rAAV5βgal). rFIVβgal and rAAV5βgal titers were $\sim 1 \times 10^8$ and 5×10^9 i.u./ml, respectively. In some experiments, a neuronal tracer, cholera toxin subunit b (CTb, List Laboratories, CA), was added at 1 μg/μl to the viral suspension. CTb is the nontoxic subunit of cholera toxin and was previously used to define the limits of an injection site in experiments with pseudorabies virus [22]. In this study, CTb immunoreactivity allowed independent visualization of cerebellar injection sites. In this manner, transport and spread of recombinant virus outside of the injection site could be distinguished from transduction within the primary injection site.

Cerebellar injections and tissue preparation: All animal procedures were approved by the University of Iowa Animal Care and Use Committee. Young adult C57BL/6 mice weighing 20–25 g were anesthetized with ketamine/xylazine. A burr hole was drilled at the midline posterior occipital bone overlying the cerebellar anterior lobe. Pressure injections (2 μl total) were made into a single cerebellar lobule using a Hamilton syringe cemented with a glass micropipette tip. A total of 16 animals were injected with rFIVβgal; eight with rFIVβgal alone, and eight with rFIVβgal plus CTb. Eight animals were injected with rAAV5βgal (four rAAV5βgal and four AAV5βgal plus CTb). Animals were sacrificed at 3–6 (rFIVβgal) or 7 (rAAV5βgal) weeks after gene transfer and cerebella, brain stems and thoracolumbar spinal cords removed. Tissues were postfixed in 4% paraformaldehyde overnight at 4°C, cryoprotected for 1–3 days in 30% sucrose in phosphate buffered saline at 4°C and then sectioned on a cryostat at 50 μm (cerebellum/brain stem sagitally and spinal cord longitudinally).

Histochemistry and immunofluorescence: Every other section was processed for β-galactosidase activity using 5-bromo-4-chloro-4-indolyl β-D-galactoside (X-Gal) according to Davidson [19,23]. Transport and spread of virus was determined by comparing the X-gal processed sections to adjacent sections that had been processed for CTb immunohistochemistry. CTb immunochemistry was performed according to Alisky and Tolbert [24]. Briefly, sections were blocked overnight in 2% rabbit serum in Tris-buffered saline, followed by 24 h in goat anti-choleragenoid (List Laboratories, Campbell, CA) diluted 1:10 000. Sections were then incubated with biotinylated, rabbit anti-goat secondary antibodies and processed using an avidin–biotin–peroxidase substrate. Neuronal versus glial transduction was determined by dual immunofluoresence for β-galactosidase (BioDesign International, Kennebunk, ME) and neuronal (calbindin) or glial (glial fibrillary acidic protein; GFAP) markers [19] on free-floating sections. Both anti-calbindin and anti-GFAP were purchased from Sigma Biochemicals (St. Louis, MO), and were used at a concentration of 1:3000 or 1:2000, respectively. Immunofluorescence was evaluated using a Zeiss LSM 510 confocal microscope and associated software.

Cell counts: β-Galactosidase-expressing Purkinje cells were counted in every other 50 μm cerebellar section under a ×10 brightfield objective. Purkinje cells were selected for quantification because they can be quickly counted in thicker sections without stereological correction [25].

RESULTS

Cerebellar injections are complicated by the fact that stereotaxic coordinates cannot be used to precisely target the site of an injection; there is animal to animal variation in the size of cerebellar lobules, as well as their 3-dimensional orientation [26]. We therefore took advantage of CTb, a reagent commonly used to track neurons from their terminals or projections to their somata. CTb allowed us two advantages: first, it enabled us to determine the exact location of the injection. Second, it revealed the pool of potentially transducable neurons at an injection site. In mice injected with virus plus CTb, CTb immunoreactivity was found encompassing the targeted cerebellar lobule (Fig. 1a,b). In some cases injections encompassed the dorsal half of one lobule and the ventral half of another lobule,

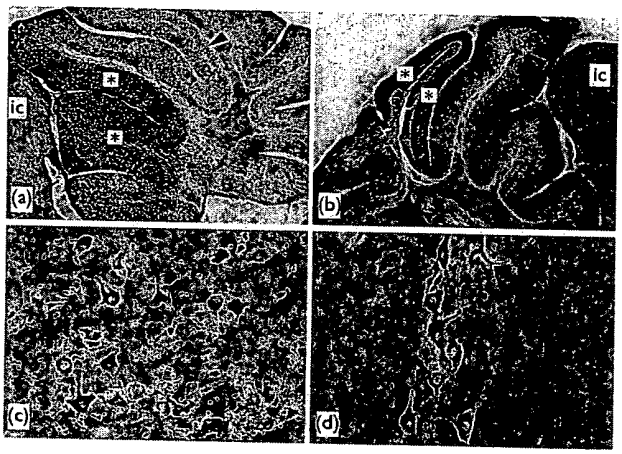

Fig. 1. Cholera toxin subunit b (CTb) injections into murine cerebella depict injection sites and retrogradely-labeled projection neurons. **(a)** Typical injection site visualized by CTb immunoreactivity. CTb is evident in the dorsal half of one lobule and the entire adjacent lobule (white asterisks). The inferior colliculus (ic) is labeled for orientation. **(b)** CTb-immunoreactivity in a section from a separate animal indicates a reduced area of exposure to CTb. The arrowheads in a and b point to mossy fiber terminals originating from cholera-labeled neurons in c and d. **(c)** Representative CTb immunoreactivity in precerebellar neurons (lateral reticular nuclei shown). **(d)** Retrogradely-labeled spinocerebellar neurons in the upper lumbar spinal cord.

while in other cases only a portion of a lobule was injected. At most, injections filled the molecular layer, Purkinje cell layer, granule cell layer and white matter of the arbor vitae but never extended to the deep cerebellar nuclei. Outside the injection site, the CTb retrogradely labeled precerebellar neurons in the cuneate, vestibular, olivary, reticular and spinal nuclei (Fig. 1c,d). Thus CTb co-injections mapped an extensive pool of neurons which could be potentially transduced via retrograde axonal transport of recombinant virus.

Recombinant FIVβgal was tested for its ability to transduce and undergo retrograde transport by cerebellar neurons. Histochemical assay for β-galactosidase activity in sections from cerebella harvested 3–6 weeks after injection of rFIVβgal into the cerebellar cortex indicated that rFIVβ gal mediated transduction to large numbers of neurons (Fig. 2a). The cytoplasmically targeted β-galactosidase was detected in the Purkinje cell somata, their dendritic arbors, and their axonal extensions (Fig. 2b,d) to the deep cerebellar and vestibular nuclei. The number of Purkinje cells transduced ranged from 78 to 1575 or 230 to 1298 in the rFIVβgal or rFIVβgal plus CTb-injected mice, respectively (Fig. 4). Thus, CTb had no profound effect on rFIV-mediated gene transfer. The number of transduced Purkinje cells was proportional to the area positive for CTb immunoreactivity. For example, in cerebella with fewer CTb-labeled neurons, there were fewer β-galactosidase-positive cells. Also, transduction was generally confined to the CTb-positive region. However, in some cerebella Purkinje cells in lobules adjacent to the injection site were also transduced.

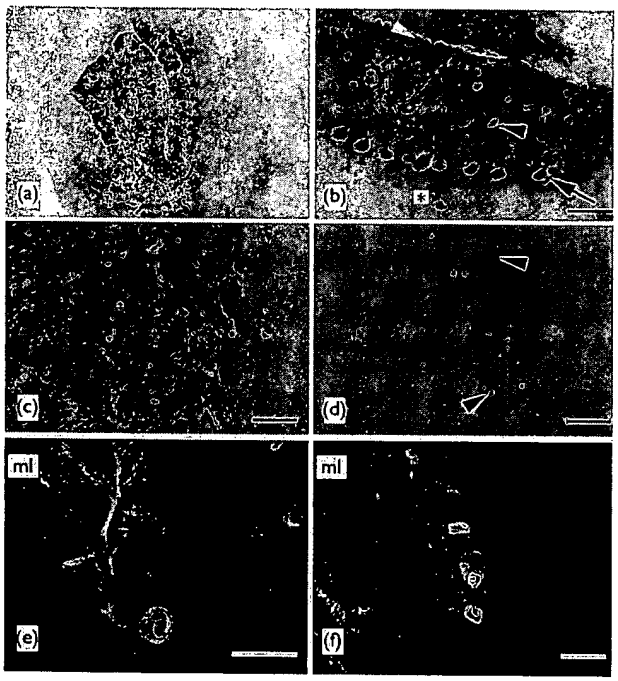

Fig. 2. rFIVβgal-mediated transduction of cells within mouse cerebellum. **(a)** Low power photomicrograph demonstrating transduction of neurons in all three cortical layers of mouse cerebellum. **(b)** Transduced row of Purkinje cells (arrow), with somata, dendritic trees and axons evident. One of the many β-galactosidase positive basket cell neurons (black arrowhead) and stellate neurons (white arrowhead) are depicted. Transduced golgi neurons within the granule cell layer are also shown (asterisk). **(c)** Transduced neurons in the deep cerebellar nuclei. **(d)** rFIVβgal mediated transduction of neurons (arrowheads) in the lateral vestibular nucleus by retrograde axonal transport of the virus from the cerebellar cortex. Purkinje cell axons are also seen. Bars in b–d = 50 μm. **(e)** Immunohistochemistry for β-galactosidase (green) and glial (red) markers show no overlap when evaluated by confocal microscopy. **(f)** Evaluation of confocal photomicrographs of sections immunostained for neuronal (red) and β-galacotosidase (green) markers demonstrate the neuronal tropism of rFIVβgal in the cerebellum. The molecular layer (ml) is noted. Bars in e and f = 30 μm.

In addition to Purkinje cells rFIVβgal transduced stellate and basket neurons in the molecular layer (Fig. 2b). In the granule cell layer, large numbers of fusiform Golgi neurons were transduced, but only scattered granule cell neurons expressed β-galactosidase (Fig. 2b). Retrograde transport of rFIVβgal was limited to deep cerebellar nuclei and lateral vestibular nuclei (Fig. 2c,d), which are the nuclei physically closest to the injection sites. Neurons in the cuneate, reticular, olivary and lumbar spinal nuclei were positive for CTb in rFIVβgal, CTb co-injected animals (Fig. 1c,d). However, these neurons were never β-galactosidase positive, indicating that rFIV has a limited ability to be retrogradely transported. Confocal microscopy of sections immunostained for neuronal or glial markers confirmed that cortical injections of FIVβgal resulted in exclusive transduction of neurons in the cortex (Fig. 2e,f).

Similar to rFIVβgal, rAAV5βgal was administered to the cerebellar cortex with or without CTb to determine the potential field of target neurons at the injection site. Again, there was no dramatic difference between rAAV5βgal plus CTb and rAAV5βgal alone, although there was much animal-to-animal variability (Fig. 4). There was extensive rAAV5βgal-mediated gene transfer to Purkinje cells, stellate and basket cells and Golgi neurons, and only minimal β-galactosidase expression in granule cell neurons (Fig. 3). The number of Purkinje cells transduced ranged from 12 to 2469 for rAAV5βgal alone and 447 to 1301 for rAAV5βgal plus CTb (Fig. 4). Evaluation of sections processed using immunohistochemistry for Purkinje or glial markers and β-galactosidase revealed that transduction was neuronal (Fig. 3e,f).

Compared with rFIVβgal, rAAV5βgal showed less retrograde transport. The only retrograde transport was to deep cerebellar nuclei (Fig. 3c). However, rAAV5βgal demonstrated greater distribution than rFIVβgal (compare Fig. 2a and Fig. 3a). Also, expressing cells could be seen in the overlying inferior colliculi (Fig. 3d). This indicates physical spread rather than axonal transport, as there are no axonal projections from the inferior colliculus into the cerebellum. This is consistent with the extensive distribution of rAAV5βgal noted following intrastriatal injections [19].

Direct counting of β-galactosidase-positive Purkinje cells in cerebella injected with rFIVβgal or rAAV5βgal give similar results (Fig. 4). Of note, the titer of rAAV5βgal was ~1 log higher than the rFIVβgal virus. Nonetheless, $>10^3$ Purkinje cells, and numerous other neurons (Fig. 2, Fig. 3) were transduced upon introduction of 10^5–10^6 i.u. rFIV or rAAV. These data indicate that both rFIV and rAAV5-based vectors efficiently transduce cerebellar neurons.

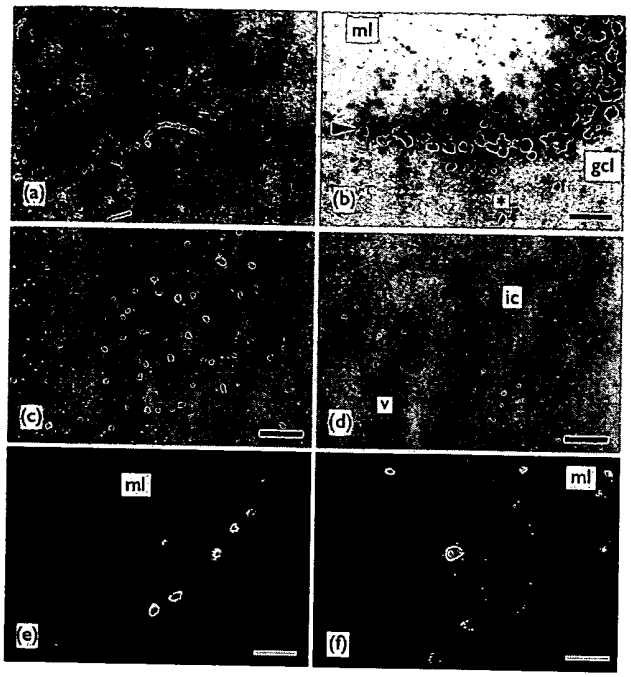

Fig. 3. rAAV5βgal-mediated gene transfer to cerebellar cells. (a) Low power photomicrograph demonstrating rAAV5βgal-mediated gene transfer to multiple lobules after a single injection. (b) Transduced nuclei of Purkinje (arrowhead) and the stellate and basket neurons in the molecular layer (ml) are easily discerned. rAAV5βgal also transduced a smaller number of Golgi neurons (asterisk) in the granule cell layer (gcl). (c) β-Galactosidase positive neurons in the deep cerebellar nuclei. (d) rAAV5βga spread outside the cerebellum to the inferior colliculi (ic). Bars in b–d = 50 μm. (e) Confocal photomicrographs following immunohistochemistry for β-galactosidase (green) and glial (red) markers show no overlap. (f) Confocal photomicrographs following immunohistochemistry for β-galactosidase (green) and Calbindin (red) markers demonstrate the Purkinje cell tropism of rAAAV5βgal in the cerebellum. Bars in e and f = 30 μm.

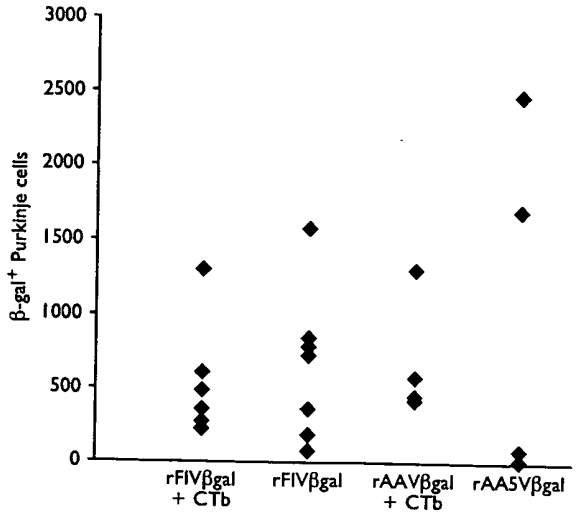

Fig. 4. Counts of transduced Purkinje cells. Each diamond represents an individual animal.

DISCUSSION

To our knowledge this is the first report of widespread direct gene transfer to cerebellar Purkinje cells. Previous reports with recombinant Ad showed limited Purkinje cell transduction mainly via retrograde transport of virus [5,6]. Our findings in the cerebellum were consistent with earlier results demonstrating transduction of cerebral neurons with recombinant lentivirus or AAV vectors [10,15–19,27]. In addition our data revealed selectivity among potential target neurons, a previously unknown characteristic of rFIV and rAAV5 vectors. This observation was probably made as a consequence of the morphologically distinct classes of neurons in each layer of the cerebellar cortex. Selective tropism could be more difficult to detect upon cerebral injection and gene transfer to the basal ganglia, because lamination and neuronal subtypes are more complex.

Within the molecular layer of a cerebellar lobule, stellate cells are located towards the outside while basket neurons are nearer the Purkinje cell bodies. The gigantic Purkinje cells form a monolayer, while fusiform Golgi neurons and small granule neurons are exclusively in the granule cell layer. Our data show that both rFIV- and rAAV5-based vectors transduce neurons in the molecular and Purkinje cell layer, with limited transduction of Golgi neurons and almost no gene transfer to granule neurons. As such we speculate that rAAV5 or rFIV vectors could be useful for studying or developing therapies for diseases in which Purkinje cells degenerate. On the other hand, these same vectors may be inappropriate for use in disorders resulting from loss of cerebellar granule cells.

The anterior lobe of the cerebellum receives input from multiple brain stem nuclei and all spinal cord segments. As such, injections into the cerebellum allow for direct evaluation of the ability of rAAV5- or rFIV-based vectors to undergo retrograde transport. We found that axonal transport with both rAAV5- and rFIV-based vectors was limited to the spatially closest nuclei. By contrast, adenovirus injected in the cerebellar cortex could be transported to the cuneate, lateral reticular and inferior olivary nuclei in the brain stem, with some limited transport to the lumbar spinal cord [5]. At this point, the inhibition of transport for rAAV5 or rFIV vectors relative to recombinant adenovirus remains unclear.

Further studies with thin sections (10–20 μm) and stereological sampling would be required for quantification of transduction of smaller neurons such as Golgi, stellate and basket cells and also to detect the small numbers of granule cells that are transduced. In this initial study, rAAV5βgal mediated transduction of the entire thickness of the molecular layer, but in the case of rFIVβgal, X-gal reaction product filled the Purkinje cell dendrites of the molecular layer, making visualization of stellate and basket cells difficult. However, our data provide an initial assessment of Purkinje cell transduction. A 2 microliter injection (10^5–10^6 i.u.) into a single lobule transduced up to 2500 Purkinje cells using rAAV5 vectors and 1500 cells using rFIV vectors. With an estimated 20000 Purkinje cells in all 10 lobules of the mouse cerebellum [28] ~10% of all Purkinje cells and close to 100% of the injected lobule (Fig. 2, Fig. 3) were transduced. With injections into multiple lobules it is reasonable to assume that most or all Purkinje cells could

ultimately be transduced with rFIV- or rAAV5-based vectors. Thus, these vectors hold promise in discerning the underlying mechanisms of degeneration in diseases where Purkinje cells degenerate, such as the human disorders SCA-2 or SCA-6, or the murine cerebellar degeneration models [3,8,28,29].

CONCLUSION

FIV and AAV5 efficiently transduce Purkinje cells and other cortical neurons with the exception of granule cells, and show promise in correction of cerebellar degeneration both hereditary and acquired.

REFERENCES

1. Kato S, Hayashi H, Mikoshiba K *et al. Acta Neuropathol* **96**, 67–74 (1998).
2. Koeppen AH. *J Neuropathol Exp Neurol* **57**, 531–543 (1998).
3. Klockgether T and Evert B. *Trends Neurosci* **21**, 413–418 (1998).
4. Paulson HL. *Am J Hum Genet* **64**, 339–345 (1999).
5. Terashima T, Miwa A, Kanegal Y *et al. Anat Embryol* **196**, 363–382 (1997).
6. Hashimoto M, Aruga J, Hosoya Y *et al. Hum Gene Ther* **7**, 149–158 (1996).
7. Vig PJ, Subramony SH, Qin Z *et al. J Neurol Sci* **174**, 100–110 (2000).
8. Lorenzetti D, Watase K, Xu B *et al. Hum Mol Genet* **9**, 779–785 (2000).
9. Poeschla EM, Wong-Staal F and Looney DJ. *Nature Med* **4**, 354–357 (1998).
10. Naldini L, Blomer U, Gallay P *et al. Science* **272**, 263–267 (1996).
11. Johnston JC, Gasmi M, Lim LE *et al. J Virol* **73**, 4991–5000 (1999).
12. Zufferey R, Nagy D, Mandel RJ *et al. Nature Biotechnol* **15**, 871–875 (1997).
13. Kordower JH, Bloch J, Ma SY *et al. Exp Neurol* **160**, 1–16 (1999).
14. Davidson BL, Brooks A, Stein CS, *et al. Mol Ther* **1**, S 250 (2000).
15. Skorupa AF, Fisher KJ, Wilson JM *et al. Exp Neurol* **160**, 17–27 (1999).
16. Bartlett JS, Samulski RJ and McCown TJ. *Hum Gene Ther* **9**, 1181–1186 (1998).
17. Lo WD, Qu G, Sferra TJ *et al. Hum Gene Ther* **10**, 201–213 (1999).
18. Mandel RJ, Rendahl KG, Spratt SK *et al. J Neurosci* **18**, 4271–4284 (1998).
19. Davidson BL, Stein CS, Heth JA *et al. Proc Natl Acad Sci USA* **97**, 3428–3432 (2000).
20. Berns KI. Parvoviridae and their replication. In: Fields BN and Knipe DM, eds. *Virology*. New York: Raven Press Ltd, 1990: 1743–1763.
21. Chiorini JA, Wendtner CM, Urcelay E *et al. Hum Gene Ther* **6**, 1531–1541 (1995).
22. Chen S, Yang M, Miselis RR and Aston-Jones G. *Brain Res* **838**, 171–183 (1999).
23. Davidson BL, Doran SE, Shewach DS *et al. Exp Neurol* **125**, 258–267 (1994).
24. Alisky JM and Tolbert DL. *J Neurosci Methods* **52**, 143–148 (1994).
25. Tolbert DL, Ewald M, Gutting J and LaRegina MC. *J Comp Neurol* **335**, 490–507 (1995).
26. Larsell O. Albino rat. In: Jansen J, ed. *The Comparative Anatomy and Histology of the Cerebellum from Monotremes Through Apes*. Minneapolis: University of Minnesota Press, 1968; 31–58.
27. Blömer U, Naldini L, Kafri T *et al. J Virol* **71**, 6641–6649 (1997).
28. Caddy KWT and Biscoe TJ. *Brain Res* **111**, 396–398 (1976).
29. Heintz N and De Jager PL. *Ann NY Acad Sci* **868**, 502–514 (1999).

Acknowledgements: Research supported by the NIH (HD33531, NS34568), Iowa Center on Aging, the Roy J. Carver Foundation (BLD), the Amyotrophic Lateral Sclerosis Association (J.A.), and the University of Iowa Center on Aging (J.A., B.L.D.). Vectors produced at the U of I Gene Transfer Vector Core. Authors thank C.I. van de Wetering and T.A. Derksen for technical assistance.

Gene Therapy (2003) 10, 34–42

www.nature.com/gt

RESEARCH ARTICLE

Viral-mediated delivery of the late-infantile neuronal ceroid lipofuscinosis gene, TPP-I to the mouse central nervous system

RE Haskell[1], SM Hughes[1], JA Chiorini[2], JM Alisky[1] and BL Davidson[1,3,4]

Program in Gene Therapy, Departments of [1]Internal Medicine, [3]Neurology, [4]Physiology & Biophysics, University of Iowa College of Medicine, Iowa City, IA, USA; [2]National Institute of Dental and Craniofacial Research, National Institutes of Health, Bethesda, MD, USA

Classical late-infantile neuronal ceroid lipofuscinosis (LINCL) is caused by mutations in tripeptidyl peptidase I (TPP-I), a pepstatin-insensitive lysosomal protease, resulting in neurodegeneration, acute seizures, visual and motor dysfunction. In vitro studies suggest that TPP-I is secreted from cells and subsequently taken up by neighboring cells, similar to other lysosomal enzymes. As such, TPP-I is an attractive candidate for enzyme replacement or gene therapy. In the present studies, we examined the feasibility of gene transfer into mouse brain using recombinant adenovirus (Ad), feline immunodeficiency virus (FIV) and adeno-associated virus (AAV) vectors expressing TPP-I, after single injections into the striatum or cerebellum. A dual TPP-I- and β-galactosidase-expressing adenovirus vector (AdTTP-I/nlsβgal) was used to distinguish transduced (β-galactosidase positive) cells from cells that endocytosed secreted TTP-I. Ten days after striatal injection of AdTTP-I/nlsβgal, β-galactosidase-positive cells were concentrated around the injection site, corpus callosum, ependyma and choroid plexus. In cerebellar injections, β-galactosidase expression was confined to the region of injection and in isolated neurons of the brainstem. Immunohistochemistry for TPP-I expression showed that TPP-I extended beyond areas of β-galactosidase activity. Immunohistochemistry for TTP-I after FIVTTP-I and AAV5TTP-I injections demonstrated TPP-I in neurons of the striatum, hippocampus and Purkinje cells. For all three vectors, TPP-I activity in brain homogenates was 3–7-fold higher than endogenous levels in the injected hemispheres. Our results indicate the feasibility of vector-mediated gene transfer of TPP-I to the CNS as a potential therapy for LINCL.
Gene Therapy (2003) **10**, 34–42. doi:10.1038/sj.gt.3301843

Keywords: *Batten disease; CLN2; gene therapy; CNS; lysosomal storage disease*

Introduction

The neuronal ceroid lipofuscinoses (NCLs) are a group of diseases related by accumulation of storage pigments in secondary lysosomes. Historically patients were classified by the ultrastructural morphology of the storage deposits and clinical course.[1,2] One type of NCL is the classical late-infantile form, late-infantile neuronal ceroid lipofuscinosis (LINCL), also known as Jansky–Bielschowsky disease and CLN2 deficiency and pepinase deficiency.[3] LINCL is an acute seizure disorder that begins between 4 and 6 years of age, with rapid deterioration in visual, motor and cognitive functioning. Lysosomal accumulations are evident by electron microscopy as curvilinear osmophilic deposits in tissue biopsies. The deposits consist predominantly of ATP synthase subunit c,[4] a hydrophobic 75 amino acid lipoprotein normally localized in the inner mitochondrial membrane. Recently, gene mapping and functional genomics has allowed identification of the disease allele, and classification of patients based on specific genetic lesions.[5]

Classical LINCL is caused by deficiency of the 46-kDa amino-tripeptidyl peptidase (TPP-I), a lysosomal serine protease with activity on peptides of less than 15 kDa.[5–8] TPP-I, which traffics via the classical mannose-6-phosphate receptor mechanism, is synthesized as a glycosylated 66 kDa inactive precursor that is auto-activated at acidic pH to remove a 20 kDa propeptide.[9] The relationship between subunit c accumulation and TPP-I deficiency is unclear, however data support a requirement for TPP-I early in the progressive enzymatic degradation of ATP synthase subunit c.[10,11]

Current therapy for LINCL can only ameliorate the seizure disorder through conventional anti-epileptic drugs, but cannot change the natural history of the disorder. This would require correcting the underlying cause of lysosomal accumulation by delivery of TPP-I, or genes expressing it, to the brain. Like the soluble lysosomal enzymes arylsulfaltase A and β-glucuronidase, TPP-I is secreted from expressing cells *in vitro*, and endocytosed into non-expressing cells.[12–14] β-Glucuronidase and arylsulfaltase A are also capable of being transported in a retrograde fashion from the site of secretion. Earlier studies in animal models of the lysosomal storage diseases metachromatic

Correspondence: BL Davidson, Roy J. Carver Professor in Internal Medicine, 200 EMRB, University of Iowa College of Medicine, Iowa City, IA 52252, USA
The first two authors contributed equally
Received 20 March 2002; accepted 2 June 2002

leukodystrophy and β-glucuronidase deficiency support the ability of directed gene expression for broadly distributed enzyme activity and correction of storage deficits.[14–19] We hypothesize that, similarly, focal TPP-I expression in brain may result in enzyme activity beyond the zone of transduced cells.

Currently, the lack of an animal model precludes testing enzyme and/or gene therapy strategies for the CNS deficits of LINCL. However, viral vectors that direct high-level expression of TPP-I allow us to make an initial assessment of enzyme spread following CNS gene transfer with recombinant adenovirus (Ad), feline immunodeficiency virus (FIV) and adeno-associated virus type 5 (AAV5) vectors. FIV results in focal transduction when delivered to brain.[19,20] Ad leads to local transduction but also moves along white matter tracts, such as the corpus callosum, for transduction of ependyma lining the ventricles.[15,16] AAV5-derived vectors infect a relatively large volume within the mouse brain.[20,21] In the current study, TPP-I wild-type mice (C57BL/6) were injected with Ad, FIV or AAV5 vectors encoding TPP-I into the striatum or cerebellum, and the levels and distribution of TPP-I assessed using immunohistochemistry and enzymatic assays.

Results

We first determined the nature of TPP-I secreted from virally transduced cells *in vitro*. A549 cells were infected with AdTPP-I, FIVTTP-I or AdnlsβgaI (control) and TPP-I activity in the media measured 48 h later. There was no measurable activity in supernatants, indicating that either TPP-I was not secreted or was secreted in the inactive form. As stated earlier, the unprocessed enzyme is inactive, with activation requiring removal of the 20 kDa pro-peptide by auto-activation at pH<4.5. Incubation of harvested supernatants in citrate buffer pH 4.2 for 30 min prior to the addition of the substrate resulted in significant increases in TPP-I activity, up to 1000 times that of the control medium. Thus, secreted TPP-I was predominantly in the inactive form (Figure 1a). In contrast, TPP-I in cell lysates was active. The 100-fold difference in cell-associated TTP-1 activity between FIV- and Ad-infected cells did not correlate to greater enzyme activity in the conditioned media of AdTTP-infected cells, suggesting that the limits of TTP-1 secretion are reached when activity approaches ~seven-fold over endogenous levels.

To determine if LINCL fibroblasts could activate exogenously derived TPP-I, a conditioned medium was

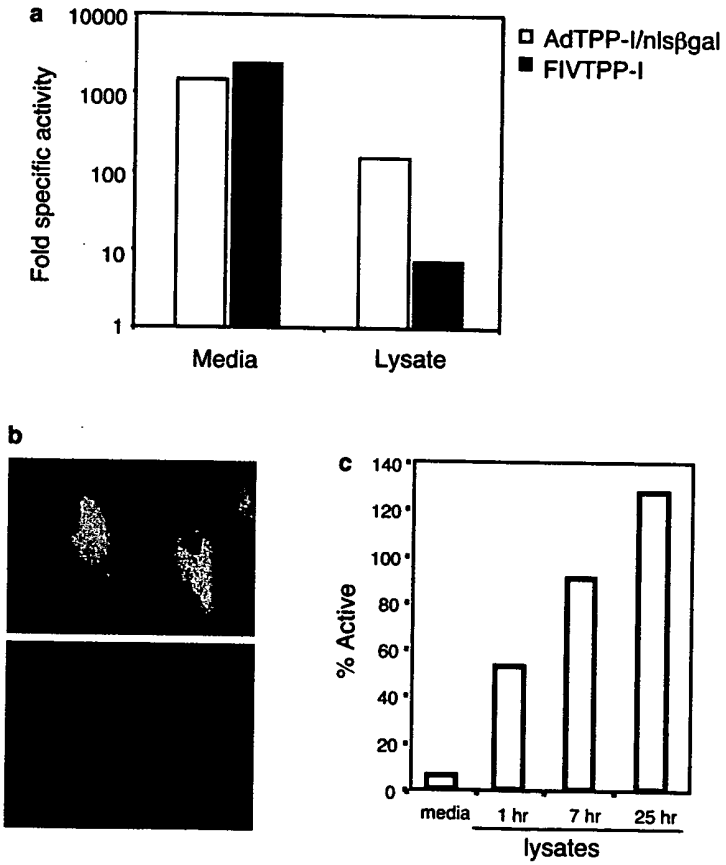

Figure 1 TPP-I activation and uptake in vitro. (a) TPP-I activity levels in cell lysates and media following infection of A549 cells with AdTPP-I/nlsβgal or FIVTPP-I, or mock infected. Enzyme activity was normalized to mock-infected A549 cells. TTP-I in media samples was autoactivated by incubation in citrate buffer pH 4.0 for 30 min. (b) LINCL cells containing a splice junction and non-sense mutation (RMO5387), immunostained 48 h after culture in TPP-I-enriched media. Cells demonstrated TPP-I immunoreactivity (top panel), in contrast to cells cultured in control media (bottom panel). (c) TPP-I activity in LINCL fibroblast cell lysates following incubation in conditioned media from AdTPP-I/nlsβgal-infected A549 cells.

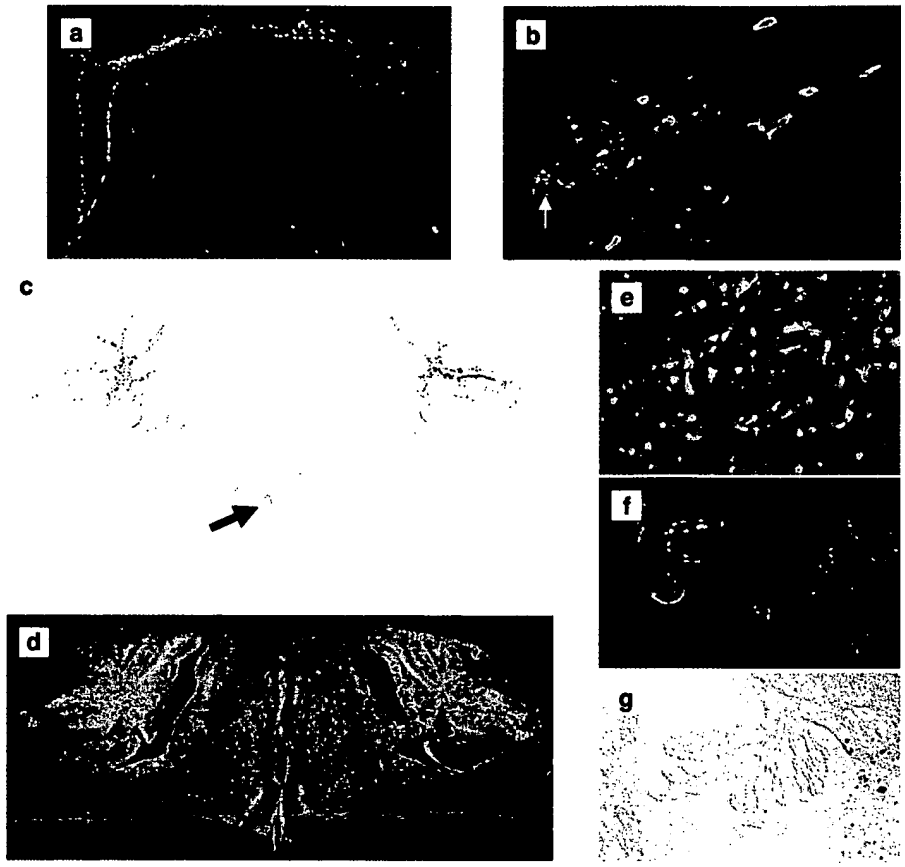

Figure 2 AdTPP-I/nlsβgal expression in the cerebrum and cerebellum 10 days post-injection. (a) Photomicrograph depicting TPP-I (green) and nlsβgal (red) immunoreactivity. (b) TPP-I-positive cells in the absence of β-galactosidase immunoreactivity (arrow) demonstrating uptake of TPP-I in the injected hemisphere. (c) β-Galactosidase expression in the cerebellum after injection of AdTTP-I/nlsβgal into the cerebellar cortex. Note the high concentration of positive nuclei primarily in the white matter tracts of the arbor vitae and also neurons in the brain stem (arrow). (d) TPP-I immunoreactivity in the section adjacent to c. (e) Dual IHC for TTP-I (green) and NeuN (red), in the brainstem. This area from c, arrow. (f) TTP-I-positive cells in the choroid plexus from d. (g) Section adjacent to F stained for β-galactosidase expression.

prepared by infecting A549 cells with AdTPP-I/nlsβgal or the control virus, Adnlsβgal. AdTPP-I/nlsβgal expressed TPP-I and nuclear-localized β-galactosidase (nlsβgal) in the E1 and E3 regions of the adenovirus genome, respectively. TPP-I and nlsβgal were expressed from the CMV or RSV promoter. LINCL fibroblasts were cultured for 48 h with conditioned or control medium from AdTPP-I/nlsβgal- or Adnlsβgal-infected A549 cells, respectively, and then stained for TPP-I immunoreactivity. TPP-I was localized to structures consistent with lysosomal/endosomal compartmentalization (Figure 1b). There was no immunoreactivity in cells treated with Adnlsβgal-conditioned supernatant. The supernatant and cell lysates were assayed 1, 7 or 25 h after addition of media (Figure 1c). Less than 10% of the TPP-I was active in the conditioned media. After 1 h, 50% of the cell-associated TPP-I was active. By 7 and 25 h, 90% and 100% of the endocytosed TPP-I was converted to active enzyme, respectively. These data demonstrate that TPP-I-deficient cells effectively endocytosed and trafficked TPP-I to acidic compartments for activation.

The secretion of TPP-I from transduced cells after injection of 7×10^9 infectious units (i.u.) of AdTTP-I into mouse brain was evaluated. The nuclear-targeted β-galactosidase allowed for identification of transduced cells (nlsβgal$^+$/TPP-I$^+$) *versus* those that had taken up TPP-I only (TPP-I$^+$/βgal$^-$). As shown in Figure 2a, IHC demonstrated TPP-I immunoreactivity in the corpus callosum, the ependyma, and the striatum following striatal injection. The majority of TPP-I-positive cells also contained β-galactosidase-positive nuclei, however some cells were clearly TPP-I$^+$/βgal$^-$ (Figure 2b, arrow) indicating that secretion and uptake had occurred. In cerebella injected with AdTPP-I/nlsβgal (2.9×10^9), β-galactosidase (Figure 2c) and TPP-I immunoreactivity (Figure 2d) were highest in the white matter tracts near the injection site. Radial projections and cell bodies of Bergman glia were also strongly positive for TPP-I immunoreactivity and β-galactosidase (not shown). Isolated βgal$^+$ cells in the brainstem (Figure 2c, arrow) were both NeuN and TPP-I positive (Figure 2e). TPP-I immunoreactivity in these cells resulted from retrograde transport of AdTPP-I/nlsβgal, rather than uptake and subsequent transport of TPP-I. TPP-I$^+$/βgal$^-$ cells were particularly notable in the choroid plexus of the 4th ventricle, indicating that these non-transduced ependymal

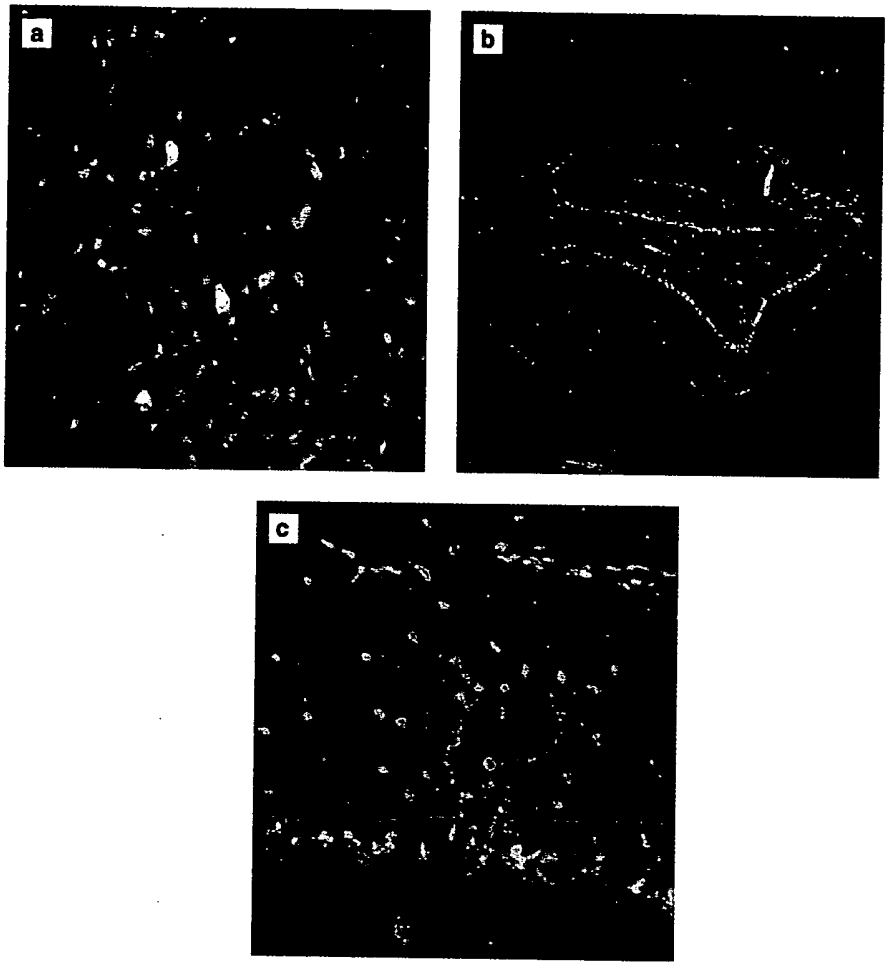

Figure 3 FIVTPP-I-mediated gene transfer to the cerebrum (a) and cerebellum (b,c). (a) TPP-I-positive, NeuN-positive cells in the striatum. (b) TPP-I immunoreactivity in Purkinje cells. (c) TPP-I staining of Purkinje cell bodies and dendrites extending into the molecular layer.

cells had endocytosed TPP-I secreted into the CSF (Figures 2f and g). Immunohistochemical analyses on naïve control brain sections were consistently negative using this rabbit polyclonal antisera (Methods).

We next tested expression from FIV- and AAV-based vectors in murine brain. In striata injected with 2.5 x 10^6 FIVTPP-I, TPP-I immunoreactivity was limited to the injection site and below the corpus callosum. Dual staining 10 days after injection demonstrated that the majority of TPP-I-positive cells were also positive for the neuronal marker NeuN (Figure 3a). Similar results were obtained at 16 and 33 weeks post-injection (not shown). Injections of FIVTPP-I (1 x 10^6 i.u) into the cerebellum resulted in TPP-I immunoreactivity in Purkinje cells and their dendrites (Figures 3b and c). For AAV5TPP-I (5 x 10^9 pt), we examined the distribution of TPP-I 10 weeks after striatal administration. TPP-I immunoreactivity was detected in sagittal brain slices several millimeters caudal to the injection site, especially in the hippocampus (Figure 4). This is consistent with earlier results showing that AAV5 transduces hippocampal neurons

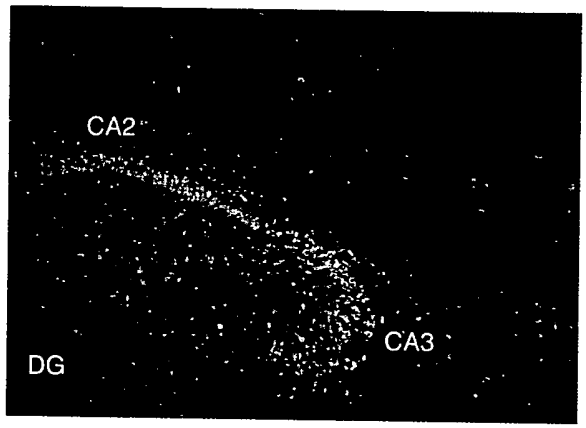

Figure 4 Expression of TPP-I 10 weeks after AAV5TPP-I injection into the cerebrum. A representative sagittal section is shown. TPP-I immunoreactivity was evident in CA2 and CA3 of the hippocampus. DG, dentate gyrus.

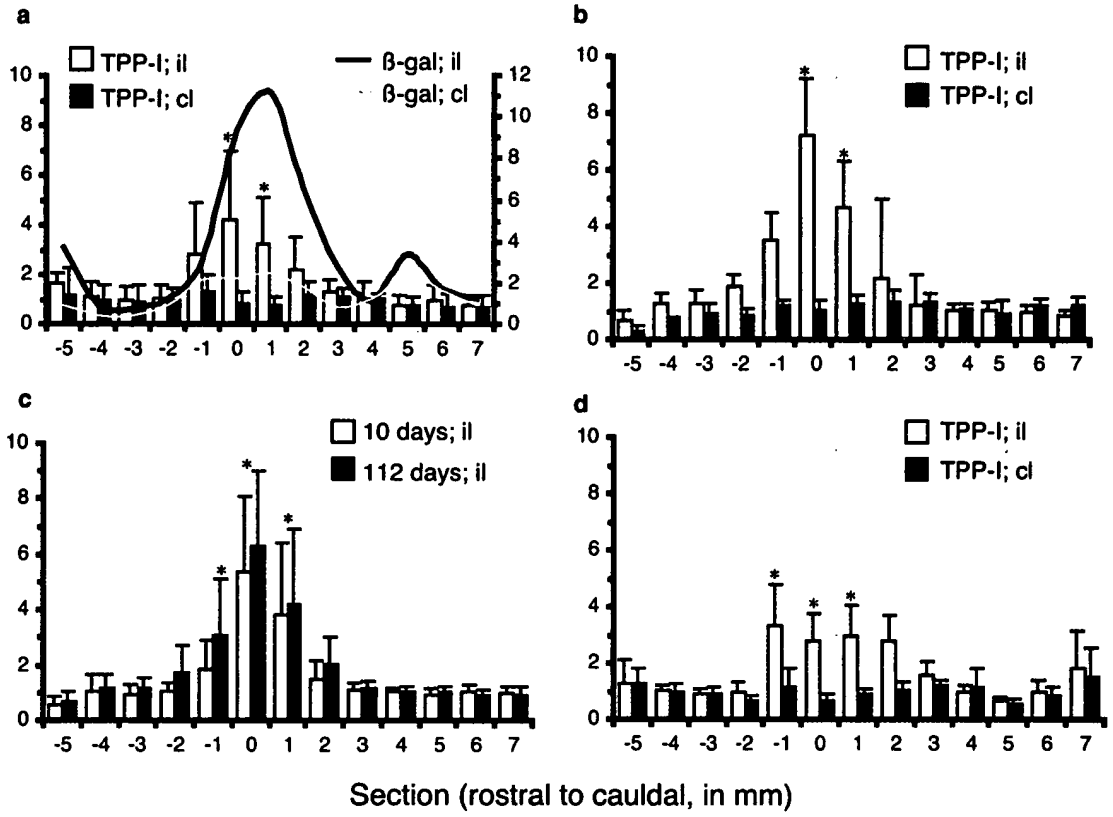

*Figure 5 TPP-I enzyme activity in brain lysates. The data are represented as fold increase in activity over non-injected controls for lysates harvested rostral (−5 mm) to caudal (7 mm) of the injection site (0 position). (a) Distribution of TPP-I and β-galactosidase 10 days after AdTTP-I/nlsβgal injection. TPP activity data are depicted as bar graphs (left y-axis, fluorescence units/mg protein). β-Galactosidase activity data are shown as line graphs (right y- axis, pg β-galactosidase/mg protein). Black line, injected (ipsilateral, il) hemisphere. Gray line, non-injected (contralateral, cl) hemisphere. (b) TPP-I activity 10 days after FIVTPP-I-mediated gene transfer. (c) Comparison of TPP-I activity in the injected hemispheres at 10 and 112 days following FIVTTP-1 gene transfer. (d) TPP-1 distribution 10 weeks after AAV5TPP-I injection into mice striata. Data represent the means ± standard deviation. In (b)–(d), y-axis is TPP-I activity (FU/mg protein). *$P \leq 0.05$ relative to control sections in all cases.*

following an intrastriatal injection (J Heth and BL Davidson, unpublished observations).

In addition to qualitative comparisons using immunohistochemistry, enzyme assays on brain lysates were done. Unlike IHC using the antibody described, endogenous levels of active TTP-I were detectable throughout the brain. At various time points after intrastriatal injection of recombinant Ad, AAV or FIV, 1-mm-thick coronal tissue slices from the entire brain were harvested and the coronal sections separated into injected (ipsilateral) and non-injected (contralateral) hemispheres. Enzyme activity in each hemisphere was independently assayed with and without pre-activation. TTP-I was in the active form as pretreatment at acidic pH did not increase levels of activity. Thus, secreted, inactive TPP-I is readily taken up and activated, or in contrast to our *in vitro* data, neural cells *in vivo* secrete TPP-I in the active form.

In mice receiving injections of 7 x 10^7 i.u. AdTPP-I/nlsβgal, TPP-I activity was up to six times higher than endogenous levels immediate to the injection site, and significantly above endogenous levels in the surrounding 4 mm ($P<0.05$ for 0 and 1 mm, respectively relative to Adβgal controls). The elevation in activity was limited to the injected hemisphere (Figure 5a). In general β-galactosidase activity correlated with TPP-I distribution, except for a consistent peak 5 mm caudal of the injection site.

FIVTPP-I injections (2.5 x 10^6 i.u.) also resulted in a similar-fold increase in TPP-I activity when compared to endogenous levels in control brain sections. At 10 days after injection, TTP-I activity was significantly higher than background within 2 mm of the injection site (Figure 5b; $P<0.05$ for 0 and 1 mm respectively, relative to control). By 16 weeks (112 days), the TPP-I activity was elevated relative to the 10 day time point, with a trend toward an increased rostral distribution (Figure 5c; $P<0.05$ for the −1, 0 and 1 mm sections, respectively relative to control). There was no further increase in enzyme levels or distribution in brains harvested and assayed 33 weeks after injection (data not shown).

Similar to AdTPP-I/nlsβgal and FIVTPP-I, AAV5TPP-I (5 x 10^9 pt) injections resulted in TPP-I enzyme activities five-fold over background. However, and unlike brains from FIVTTP-I injected mice, AAV5TPP-I did not result in a distinct peak of TPP-I activity. We found elevated, nearly equivalent levels of enzyme 4 mm around the injection site (Figure 5d) which was significantly greater

than control treated mice ($P<0.05$ for–1, 0 and 1 mm sections, respectively). Together, the data support that TPP-I can be expressed in brain following transduction of neurons, glia and ependyma, with spread of enzyme detectable up to 4 mm surrounding the injection site.

Discussion

Delivery of TPP-I to cells in the CNS by viral-mediated gene delivery may provide therapy for LINCL. Amelioration of the CNS deficits of this disorder would likely require widespread, rather than focal correction. Using other animal models of lysosomal storage disease as guides,[14,15,19,22] we hypothesize that TPP-I secretion from transduced cells, followed by subsequent uptake by non-transduced cells, would lead to an extensive area of recombinant enzyme activity. In the current study we found that TPP-I expressed in brain is secreted and active, and using IHC and enzyme assay found evidence of TPP-I 2–4 mm from the injection site. While the sensitivity of our assays precludes the detection of increased enzyme expression beyond this region, we believe that the spread of enzyme may extend beyond the 2–4 mm detected. The best assessment of the extent of enzyme spread and correction will come from studies performed in animals deficient in TPP-I.

Similar to earlier work with TPP-I harvested from baculovirus-infected Sf9 cells, or overexpressing COS cells,[9] TPP-I secreted from A549 cells was inactive. In both cases, the enzyme could be auto-activated *in vitro* at pH<4.5, or alternatively, following endocytosis by LINCL fibroblasts and lysosomal activation. Surprisingly, we did not find evidence of inactive enzyme in brains following viral-mediated gene transfer of TPP-I. Pre-activation of tissue lysates at low pH did not enhance TTP-I activity levels, and the kinetics of each reaction were linear over the entire assay, indicating that essentially all of the TPP-I in the brain was in the active form. Our *in vitro* data support that TPP-I was secreted as the inactive 66 kDa form *in vivo* followed by immediate uptake and activation.

We were surprised to find few transduced TTP-I$^+$/βgal$^-$ cells given our prior experience with β-glucuronidase, and data from other published reports. This may reflect distinct differences between TPP-I and the lysosomal enzymes α-*N*-acetylglucosaminidase, arylsulfatase A, and β-glucuronidase with respect to their ability to spread from the site of secretion. Alternatively, it could reflect the sensitivity of our enzyme activity assay method, or the polyclonal antibody. The best indication of TPP-I spread, either through retrograde transport or by distribution through the CSF, will come from TPP-I-knock-out mice with a measurable and/or histological phenotype where issues of clearance of pathology relative to enzyme activity levels can be addressed.

The vectors used in this study resulted in a three- to seven-fold increase over endogenous TPP-I activity following a single injection, and TPP-I distribution increased from 10 days to 16 weeks in mice injected with FIVTPP-I. In AAV5 and FIV, two vectors known to provide long-term expression, these levels were maintained until the end of the experiment at 10 and 33 weeks respectively. The levels of TPP-I activity required for therapeutic benefit are currently unknown. Using other lysosomal disorders as a benchmark, generally 1–5% normal enzymatic levels are sufficient for beneficial effects by enzyme replacement therapies.[23–25] Again, therapeutic levels of TPP-I that are undetectable by IHC or enzyme assay, may be sufficient for correction of the cellular phenotype, as seen in the mucopolysaccharidosis type VII mouse model.[13,16,26]

Increased β-galactosidase activity in the region 5 mm caudal to the injection site in AdTPP-I-injected mice did not result in detectable local increases in TPP-I activity (Figure 5a). These cells were presumably infected at their termini followed by retrograde transport of the vector, leading to increased β-galactosidase activity. Lack of detectable TTP-I in these same cells could be due to assay sensitivity limits. An alternative possibility is that TPP-I was made in these cells with most anterogradely transported back to the injection site.

Injection of adenovirus into the cerebellum gave the most convincing evidence of secretion and uptake of TPP-I. Cells of the choroid plexus were very positive for TPP-I immunoreactivity but displayed no detectable β-galactosidase activity. Interestingly, expression of TPP-I in Bergman glia did not lead to TPP-I immunoreactivity in Purkinje cells. This may indicate that either Bergman glia do not secrete TPP-I, or that the nearby Purkinje cell soma and its extensive dendritic tree do not efficiently endocytose TPP-I.

In summary, the total distribution of TPP-I is the product of the intrinsic ability of the vector to spread from the injection site and the subsequent spread of the secreted gene product. Optimization of the efficiency of TPP-I delivery will require the use of vectors that demonstrate wide distribution and long-term expression. In addition, modifications of the secreted proteins may be employed to increase their ability to spread throughout the parenchyma.[13] Maximizing distribution of the vectors or the specific gene product will facilitate effective therapies for LINCL and other lysosomal storage diseases.

Materials and methods

Viral constructs

An adenovirus encoding TPP-I in the E1 region was generated by sub-cloning the human TPP-I cDNA[12] into the pacAd5CMV plasmid. The resulting shuttle (Ad5CMVTPP-I) was recombined with pacAd5 9.2-100 in HEK 293 cells to produce recombinant adenovirus particles, AdTTP-I.[27] The second adenovirus used in this study contained a nuclear targeted lacZ (nlsβgal) subcloned into the E3 region in addition to TPP-I in E1. To generate this construct, the existing pacAd5 9.2-100 plasmid was modified to include a SwaI restriction site after deleting the E3 region.[13] DNA containing nlsβgal was cut from the plasmid pAdCMVnlsβgal with PmeI and SpeI and sub-cloned into the pAd5E3RSV recombination shuttle. Ad5E3RSVnlsβgal was cut with SfuI and Ad5 9.2-100SwaI with SwaI and recombined using methods described earlier.[13,28] The resulting plasmid pacAd5 9.2-100nlsβgal was then transfected with the Ad5CMVTPP-I shuttle in HEK 293 cells to make the dual-expressing virus Ad5TPP-I/nlsβgal.[27] Adenoviruses were purified by the University of Iowa Gene

Transfer Vector Core by CsCl gradient purification and titered by plaque assay on A549 and HEK 293 cells.

For FIV constructs, the TPP-I cDNA was cloned into the pVETLRSVmcs FIV genome plasmid.[29] The TPP-I-containing plasmid was combined with pCFIVΔorfΔvif and pCMV-G in a triple transfection in HT 1080 cells.[19,29] The medium was collected over a 4-day period, passed through a 0.45 μM filter and centrifuged at 7500 *g* to concentrate the retrovirus particles. The pellet was then resuspended in 1 mL lactose buffer (40 mg/ml lactose in PBS). Viral titers of FIVTPP-I were estimated by infecting A549 cells with serial dilutions of the viral stock followed by immunohistochemistry for TPP-I. FIV particles were generated in the University of Iowa Gene Transfer Vector Core.

Recombinant AAV5 vectors were produced by triple transfection of the TPP-I expression cassette, containing the native AAV5 ITR and the Rous Sarcoma virus long terminal repeat promoter, a plasmid containing AAV5 rep and cap, and a third plasmid containing helper function from adenovirus type 5. Recombinant AAV5TPP-I was purified as described previously and titered by quantitative PCR.[20,30,31] The viral titer was 1.0 x 10^{12} genome copies (particles)/ml. AAV5TPP-I was dialyzed against lactated Ringer's solution prior to injection.

Animals and injections

Six-week-old C57Bl/6 mice were purchased from Jackson Labs (Bar Harbor, ME, USA) and housed at the University of Iowa Animal Care Facility. The University of Iowa Animal Care and Use Committee approved all animal procedures. For striatal injections, mice were injected at coordinates 0.4 mm rostral, 2 mm lateral from the bregma, at a depth of 3 mm with 5 μl injections of one of the following viruses: 7.0 x 10^7 i.u. of AdTPP-I/nlsβgal (n=12), 2.5 x 10^6 i.u. of FIVTPP-I (n=14) or 5 x 10^9 pt of AAV5TPP-I (n=6). For cerebellar injections, 2 μl of virus containing 2.8 x 10^9 i.u. of AdTPP-I/nlsβgal (n=3) or 1 x 10^6 i.u. of FIVTPP-I (n=3) was injected into the anterior cerebellar lobe underlying the midline posterior occipital bone using a Hamilton syringe cemented with a glass micropipette tip.[20] Control animals either received no injection (n=4), or were injected with Ad5nlsβgal (n=4).

Tissue harvest and processing

All animals injected with adenovirus and FIV were evaluated 10 days after injection (n=6 each) and AAV5 animals at 10 weeks (n=5). Mice injected with FIV animals were also evaluated at 16 weeks (n=4) and 33 weeks (n=3).

For cryostat sections and immunohistochemistry, animals were perfused with 2% paraformaldehyde. Brains were removed and post-fixed 2 h in 2% paraformaldehyde, cryoprotected overnight in 30% sucrose, embedded in OCT and sectioned on a cryostat at 10 μm for subsequent immunostaining.

For enzyme assays, mice were euthanized and the brains removed, cut rostral to caudal at 1 mm intervals and hemispheres separated for analysis. Samples were frozen immediately in liquid N_2 and extracts prepared by homogenization in 500 μl of ice-cold lysis buffer (0.15 M NaCl, 0.1% Triton X-100). Nuclei and cellular debris were pelleted at 10 000 *g* at 4°C. The soluble fraction was removed and saved for TPP-I analysis. Nuclear pellets from Ad-injected mice were retained for β-galactosidase activity and were sonicated for 10 s in 500 μl of lysis solution. All samples were frozen at −80°C until assayed. Protein concentrations were determined by the DC protein assay (BioRad, Hercules, CA, USA).

TPP-I antibody and immunohistochemistry

Antibodies against TPP-I were generated by injecting rabbits with 500 μl of 1 x 10^{12} pt/ml of AdTPP-I into four intramuscular and one intradermal site. The rabbits were boosted with the same dosage and routes 2 weeks later. Serum aliquots were stored at−20°C. Rabbit serum was tested for TPP-I specific antibodies by immunostaining (1) transfected cells containing expression plasmids devoid of all adenovirus sequences, (2) cells infected with FIVTPP-I, and (3) tissue sections from mice injected with adenovirus expressing human β-glucuronidase and nuclear-targeted β-galactosidase (Adβgluc/nlsβgal). Antibodies directed against TPP-I were detected in TPP-I-expressing tissues and cells but not in Adβgluc/nlsβgal-injected mice. Rabbit anti-TPP-I serum was used at 1:600. To detect neurons, mouse anti-NeuN 1:100 (Chemicon International Inc., Temecula, CA, USA) directly conjugated to Alexa 568 (Molecular Probes, Eugene, OR, USA) was used. Polyclonal rabbit anti-β-galactosidase (BioDesign International, Sao, MN, USA), directly conjugated to Alexa 568 and diluted 1:1500 was used to detect cells infected with adenovirus. All antibodies were diluted in 3% BSA, 0.1% saponin, 0.3% Triton X-100 in PBS (diluent). After blocking tissue sections for 30 min in diluent containing 10% serum, samples were incubated with primary antibodies overnight at 4°C. Samples were washed extensively in diluent and stained with fluorescently labeled secondary antibodies for 2 h at room temperature. Photomicrographs were captured using Adobe Photoshop and a SPOT/RT digital camera (Diagnostic Inst, Sterling Heights, MI, USA) on a Leica DMRBE fluorescent microscope or Olympus IX70 inverted microscope.

LINCL fibroblasts

LINCL fibroblasts previously isolated from patients were kindly provided by Dr Peter Lobel (Rutgers University, Piscataway, NJ, USA). Compound heterozygous fibroblasts that contained a G3560C splice junction mutation and a C3674T non-sense mutation in *TPP-I* were used to evaluate the ability of these deficient cells to sequester and activate TPP-I expressed from viral vectors. Fibroblasts were grown in DMEM supplemented with 10% FCS plus pen/strep. Fibroblasts were cultured in media containing 2% FCS, DMEM and 10 MOI of AdTPP-I/nlsβgal added for 4 h, followed by removal of virus. Cells were cultured for an additional 48 h before TPP-I activity assays were done on media and cell lysate fractions. To test for TTP-I uptake, A549 cells were infected at an MOI of 50 in DMEM containing 2% FCS, DMEM for 4 h, followed by virus removal and an additional 48 h culture. The medium was removed 48 h after infection and added to patient fibroblast cultures in six-well plates. Media and cells were harvested and TPP-I activity measured. For immunohistochemistry, patient cells were cultured for 48 h in TPP-I-enriched media harvested from virally infected A549 cells and then stained with anti-TPP-I.

Enzyme activity assays

β-Galactosidase and TPP-I enzyme activities were analyzed in a 96-well fluorescence microplate reader (BMG Technologies, Durham, NC, USA) with Costar 3631 plates (Fisher Scientific, Pittsburgh, PA, USA). TPP-I activity was measured at 37°C using the substrate Ala–Ala–Phe 7-amido-4-methylcoumarin (AAF-AMC; Sigma St. Louis, MO, USA) at 380 nm excitation, 460 nm emission.[32] Prior to assay, samples were either maintained at neutral pH or pre-activated by incubation in citrate buffer (0.15 M NaCl, 0.05 M sodium citrate pH 4.2) for 20 min. Plates were pre-warmed to 37°C prior to the addition of substrate (50 µl of 400 µM AAF-AMC in citrate buffer). Samples were read every 2 min for 30 min. TPP-I activities from all mice were expressed as fluorescent units per minute per mg protein. Endogenous TTP-I activities from non-injected control mice were used to determine fold increase in expression after viral injections.

β-Galactosidase activities were measured in the nuclear fraction of all adenovirus-injected mice using the FluoReporter *lacZ* Quantitation Kit (Molecular Probes, Eugene, OR, USA) in accordance with the manufacturer's directions. Standard curves were generated using 0.02–5 ng purified β-galactosidase (Sigma, St. Louis, MO, USA). Aliquots of 5 µl of nuclear extract or β-galactosidase were incubated with 1.1 mM 3-carboxy-umbelliferyl β-D-galactopyranoside in reaction buffer (0.1 M sodium phosphate, pH 7.3, 1 mM magnesium chloride and 45 mM β-mercaptoethanol) for 30 min at room temperature. Stop buffer (0.2 M Na_2CO_3) was added and the fluorescent product measured at 380 nm excitation and 460 nm emission. Emission values were converted to pg β-galactosidase per mg protein based on β-galactosidase standard curves and sample protein concentrations.

Acknowledgements

The authors thank Dr Istvan Sohar and Dr Peter Lobel for assistance with the TPP-I activity assays, Dr Sybille Sauter for the FIVTPP plasmid, Inês Martins and Ken Ratliff for excellent technical assistance and Drs Colleen Stein and Jason Heth for critical discussions. We also thank the University of Iowa Gene Transfer Vector Core (DK 54759) for help with virus production. This work was supported in part by a grant from the Batten Disease Support and Research Association (BDSRA), and from the Roy J. Carver Trust (BLD).

References

1 Opitz JM. *Ceroid-lipofuscinoses. Batten Disease and Allied Disorders.* Alan R. Liss, Inc.: New York, 1987,pp 1–307.
2 Goebel HH, Mole SE, Lake BD. *The Neuronal Ceroid Lipofuscinoses (Batten Disease): Biomedical and Health Research.* IOS Press: Amsterdam, 1999, p 33.
3 Sohar I, Sleat DE, Jadot M, Lobel P. Biochemical characterization of a lysosomal protease deficient in classical late infantile neuronal ceroid lipofuscinosis (LINCL) and development of an enzyme-based assay for diagnosis and exclusion of LINCL in human specimens and animal models. *J Neurochem* 1999; **73**: 700–711.
4 Palmer DN *et al*. Mitochondrial ATP synthase subunit c storage in the ceroid-lipofuscinoses (Batten disease). *Am J Med Genet* 1992; **42**: 561–567.
5 Sleat DE *et al*. Association of mutations in a lysosomal protein with classical late-infantile neuronal ceroid lipofuscinosis. *Science* 1997; **277**: 1802–1805.
6 Vines D, Warburton MJ. Purification and characterisation of a tripeptidyl aminopeptidase I from rat spleen. *Biochim Biophys Acta* 1998; **1384**: 233–242.
7 Rawlings ND, Barrett AJ. Tripeptidyl-peptidase I is apparently the CLN2 protein absent in classical late-infantile neuronal ceroid lipofuscinosis. *Biochim Biophys Acta* 1999; **1429**: 496–500.
8 Vines DJ, Warburton MJ. Classical late infantile neuronal ceroid lipofuscinosis fibroblasts are deficient in lysosomal tripeptidyl peptidase I. *FEBS Lett* 1999; **443**: 131–135.
9 Lin L, Sohart I, Lackland H, Lobel P. The human CLN2 protein/tripeptidyl-peptidase I is a serine protease that autoactivates at acIdic pH. *J Biol Chem* 2001; **276**: 2249–2255.
10 Ezaki J, Takeda-Ezaki M, Kominami E. Tripeptidyl peptidase I, the late infantile neuronal ceroid lipofuscinosis gene product, initiates the lysosomal degradation of subunit c of ATP synthase. *J Biochem* 2000; **128**: 509–516.
11 Ezaki J, Tanida I, Kanehagi N, Kominami E. A lysosomal proteinase, the late infantile neuronal ceroid lipofuscinosis gene (CLN2) product, is essential for degradation of a hydrophobic protein, the subunit c of ATP synthase. *J Neurochem* 1999; **72**: 2573–2582.
12 Lin L, Lobel P. Production and characterization of recombinant human CLN2 protein for enzyme-replacement therapy in late infantile neuronal ceroid lipofus. *Biochem J* 2001; **357**: 49–55.
13 Xia H, Mao Q, Davidson BL. The HIV Tat protein transduction domain improves the biodistribution of β-glucuronidase expressed from recombinant viral vectors. *Nat Biotechnol* 2001; **19**: 640–644.
14 Consiglio A *et al*. *In vivo* gene therapy of metachromatic leukodystrophy by lentiviral vectors: correction of neuropathology and protection against learning impairments in affected mice. *Nat Med* 2001; **7**: 310–316.
15 Ghodsi A *et al*. Extensive β-glucuronidase activity in murine CNS after adenovirus mediated gene transfer to brain. *Hum Gene Ther* 1998; **9**: 2331–2340.
16 Stein CS, Ghodsi A, Derksen T, Davidson BL. Systemic and central nervous system correction of lysosomal storage in mucopolysaccharidosis type VII mice. *J Virol* 1999; **73**: 3424–3429.
17 Vogler C *et al*. Murine mucopolysaccharidosis type VII: the impact of therapies on the clinical course and pathology in a murine model of lysosomal storage disease. *J Inherit Metab Dis* 1998; **21**: 575–586.
18 Bosch A *et al*. Reversal of pathology in the entire brain of mucopolysaccharidosis type VII mice after lentivirus-mediated gene transfer. *Hum Gene Ther* 2000; **11**: 1139–1150.
19 Brooks AI *et al*. Functional correction of established CNS deficits in an animal model of lysosomal storage disease using feline immunodeficiency virus-based vectors. *Proc Natl Acad Sci USA* 2002; **99**: 6216–6221.
20 Alisky JM *et al*. Transduction of murine cerebellar neurons with recombinant FIV and AAV5 vectors. *NeuroReport* 2000; **11**: 2669–2673.
21 Davidson BL *et al*. Recombinant AAV type 2, 4, and 5 vectors: transduction of variant cell types and regions in the mammalian CNS. *Proc Natl Acad Sci USA* 2000; **97**: 3428–3432.
22 Fu H *et al*. Neurological correction of lysosomal storage in a mucopolysaccharidosis IIIB mouse model by adeno-associated virus-mediated gene delivery. *Mol Ther* 2002; **5**: 42–49.
23 Barranger JA, O'Rourke E. Lessons learned from the development of enzyme therapy for Gaucher disease. *J Inherit Metab Dis* 2001; **24**: 89–96.

24 Desnick RJ, Banikazemi M, Wasserstein M. Enzyme replacement therapy for Fabry disease, an inherited nephropathy. *Clin Nephrol* 2002; **57**: 1–8.
25 Leone P, Janson CG, McPhee SJ, During MJ. Global CNS gene transfer for a childhood neurogenetic enzyme deficiency: Canavan disease. *Curr Opin Mol Ther* 1999; **1**: 487–492.
26 Ghodsi A *et al*. Systemic hyperosmolality improves β-glucuronidase distribution and pathology in murine MPS VII brain following intraventricular gene transfer. *Exp Neurol* 1999; **160**: 109–116.
27 Anderson RD *et al*. A simple method for the rapid generation of recombinant adenovirus vectors. *Gene Ther* 2000; **7**: 1034–1038.
28 Chartier C *et al*. Efficient generation of recombinant adenovirus vectors by homologous recombination in *Escherichia coli*. *J Virol* 1996; **70**: 4805–4810.
29 Johnston JC *et al*. Minimum requirements for efficient transduction of dividing and nondividing cells by feline immunodeficiency virus vectors. *J Virol* 1999; **73**: 4991–5000.
30 Chiorini JA *et al*. High-efficiency transfer of the T cell co-stimulatory molecule B7-2 to lymphoid cells using high-titer recombinant adeno-associated virus vectors. *Hum Gene Ther* 1995; **6**: 1531–1541.
31 Davidson BL, Chiorini JA. Recombinant adeno-associated virus vector types 4 and 5: preparation and application for CNS gene transfer. *Viral Vectors Gene Ther* 2003 (in press).
32 Page AE, Fuller K, Chambers TJ, Warburton MJ. Purification and characterization of a tripeptidyl peptidase I from human osteoclastomas: evidence for its role in bone resorption. *Arch Biochem Biophys* 1993; **306**: 354–359.